Tris(oxalato) Complexes of Silicon as Precursors to Porous Silicate Materials: Synthesis and Structure

Kenneth J. Balkus, Jr.,*,† Irina S. Gabrielova,† and Simon G. Bott*,‡

Departments of Chemistry, University of Texas at Dallas, Richardson, Texas 75083-0688, and University of North Texas, Denton, Texas 76203

Received May 5, 1995[⊗]

A series of alkylammonium tris(oxalato)silicate compounds $[R_4N]_2[Si(C_2O_4)_3]$, where $R_4N^+ = (CH_3)_4N^+$ (**1**), $(CH_3)_3(C_6H_5)N^+$ (**2**), $(CH_3CH_2)_4N^+$ (**3**), $(CH_3CH_2CH_2)_4N^+$ (**4**), $(CH_3(CH_2)_3)_4N^+$ (**5**), and $(CH_3(CH_2)_5)_4N^+$ (**6**), were prepared as precursors to microporous materials. Compounds **1** and **2** were structurally characterized by X-ray crystallography. $[(CH_3)_4N]_2[Si(C_2O_4)_3]$ and $[(CH_3)_3(C_6H_5)N]_2[Si(C_2O_4)_3]$ crystallize in the monoclinic $P2_1/c$ and $P2_1/n$ space groups respectively with $a = 17.631(2)$ Å, $b = 10.1984(9)$ Å, $c = 12.095(1)$ Å, $\beta = 108.810(8)°$, and $Z = 4$ for **1** while $a = 8.855(2)$ Å, $b = 18.050(2)$ Å, $c = 17.102(2)$ Å, $\beta = 95.24(1)°$, and $Z = 4$ for **2**. The oxalate (ox) ligands are arranged in an octahedral fashion around the silicon. Thermal decomposition of the oxalate complexes **1**−**6** results in amorphous silica. Single point determination of the surface area indicates a greater surface area is obtained as the size of the alkylammonium ions increases.

Introduction

Although the oxalate ion (ox) is a fairly ubiquitous ligand, interesting coordination chemistry continues to emerge. The oxalate ion can function as a bridging chelate, which could result in polymeric or network type structures. Recently, certain metal oxalato complexes have been shown to form two- and three-dimensional microporous materials.[1] The presence of channels and occluded guest molecules in these structures is reminiscent of zeolite molecular sieve frameworks.[2] As a result, we became intrigued with the idea that maybe we could prepare a silicon oxalate complex having a network type structure and that upon thermal decomposition the resulting oxide would be predisposed toward a microporous material having specific pore dimensions. Therefore, as part of a preliminary study we prepared a series of tris(oxalato)silicate complexes having different alkyl ammonium ions to balance the charge. Aliphatic amines are popular templates or structure directing agents in zeolite synthesis. We anticipated that the size and shape of the ammonium ion might also influence the structure of the silicon oxalate and subsequent oxide materials. The crystal structure of a tris(oxalato)silicate had not been previously reported. Therefore, we determined the structure of tetramethylammonium tris(oxalato)silicate, **1**, and phenyltrimethylammonium tris(oxalato)silicate, **2**, by single-crystal X-ray diffraction. Additionally, other $[R_4N]_2[Si(C_2O_4)_3]$ (where R = ethyl, *n*-propyl, *n*-butyl, and *n*-hexyl) complexes, **3**−**6**, were synthesized and characterized spectroscopically. The oxalate complexes were then thermally decomposed to form silica. Heating triethylammonium tris(oxalato)silicate at 400 °C was recently reported[3] to yield amorphous silica. Similarly, heating complexes **1**−**6** results in amorphous silica. However, the surface areas of the resulting silica appear to increase with the size of the ammonium ion. This lends support to the premise that the alkylammonium ion acts as a void filler and regulates the pore dimensions of the silica.

Experimental Section

Alkylammonium salts and silicon tetrachloride were obtained from Aldrich and used without further purification. Acetone was dried over 4 Å molecular sieves prior to use. Silver oxalate was freshly prepared for each synthesis by mixing 12.13 g (0.066 mol) of potassium oxalate dissolved in 150 mL of deionized water and 22.37 g (0.132 mol) of silver nitrate dissolved at room temperature in 250 mL of deionized water in a Kimax red glass flask (Fisher) that excludes light below 500 nm. The white precipitate was suction filtered and dried in vacuo at 60 °C with an average yield 96%. (CAUTION: Silver oxalate will explode at 140 °C and should be heated carefully. Silver oxalate is also light sensitive and should be stored in a dark place.)

$[(CH_3)_4N]_2[Si(ox)_3]$ (1). The preparation of tetramethylammonium tris(oxalato)silicate, **1**, is similar to the literature procedure.[5] First 4.83 g of $Ag_2C_2O_4$ (excess) and 300 mL of dry acetone were mixed in a red glass flask with stirring for 10 min. Then 1.13 g (0.01 mol) of $(CH_3)_4NBr$ and 0.59 mL (0.005 mol) of $SiCl_4$ were added. The flask was covered with aluminum foil to exclude light, and the mixture was stirred for an additional hour. The contents of the flask were suction filtered to remove the silver salts. Anhydrous ether (~400 mL) was added to the filtrate which resulted in precipitation of the crude product. The colorless crystals were suction filtered and then redissolved in absolute ethanol. The silicon oxalate solution was gravity filtered and then allowed to evaporate to dryness. Crystals of **1** were isolated with a 65% yield. FT-IR: 1761 (s), 1684 (w), 1347 (s), 1247 (m), 915 (ms), 858 (ms), 827 (ms), 651 (s), 625 (m), 569 (s), and 498 (m) cm^{-1}.

$[(CH_3)_3(C_6H_5)N]_2[Si(ox)_3]$ (2). Phenyltrimethylammonium tris(oxalato)silicate, **2**, was prepared by first combining 4.79 g of $Ag_2C_2O_4$ (excess) with 300 mL of dry acetone in a red glass flask. After ~10 min of stirring 1.733 g (0.01 mol) of $(CH_3)_3(C_6H_5)NCl$ and 0.58 mL (0.005 mol) of $SiCl_4$ were added. The mixture was stirred for 1 h as the silver halides precipitated. The slurry was suction filtered and the filtrate was diluted with ~400 mL of anhydrous ether. The resulting

† University of Texas at Dallas.
‡ University of North Texas.
⊗ Abstract published in *Advance ACS Abstracts,* November 1, 1995.

(1) For example, see: Decurtins, S.; Schmalle, H. W.; Schneuwly, P.; Oswald, H. R. *Inorg. Chem.* **1993**, *32*, 1888. Farrel, R. P.; Hambley, T. W.; Lay, P. A. *Inorg. Chem.* **1995**, *34*, 757. De Munno, G.; Ruiz, R.; Lloret, F.; Faus, J.; Sessoli, R.; Julve, M. *Inorg. Chem.* **1995**, *34*, 408.
(2) For an overview, see: Szostak, R. *Molecular Sieves*, Van Nostrand Reinhold: New York, 1989.
(3) Ferracin, L. C.; Ionashiro, M.; Davolos; M. R. *An. Congr. Bras. Ceram., 34th* **1990**, 203.
(4) Dean, P. A. W.; Evans, D. F.; Phillips, R. F. *J. Chem. Soc. A* **1969**, 363.
(5) Schott, V. G.; Lange, D. Z. *Anorg. Allg. Chem.* **1972**, *391*, 27.

0020-1669/95/1334-5776$09.00/0

precipitate was isolated by suction filtration and then redissolved in absolute ethanol. The ethanol solution was gravity filtered and then evaporated to dryness. The resulting colorless crystals of **2** were obtained in 55% yield. FT-IR: 1760 (s), 1677 (m), 1337 (s), 1238 (ms), 910 (ms), 854 (ms), 829 (ms), 646 (s), 622 (ms), 566 (s), and 497 (m) cm^{-1}.

$[(CH_3CH_2)_4N]_2[Si(ox)_3]$ (3). The synthesis of tetraethylammonium tris(oxalato)silicate, **3**, was conducted in a manner similar to the published procedure.[4] A 4.73 g sample of freshly prepared $Ag_2C_2O_4$ (excess) were mixed with 300 mL of dry acetone in a red glass flask. Then 0.41 mL (0.0036 mol) of $SiCl_4$ and 1.52 grams (0.0072 mol) of $(CH_3CH_2)_4NBr$ were added. The mixture was stirred for 1 h during which the silver halides precipitated. The slurry was suction filtered, and anhydrous ether was added to the filtrate. Crystals of the crude product **3** were isolated by suction filtration and then redissolved in absolute ethanol. The solution was gravity filtered and allowed to evaporate to dryness. Colorless crystals of **3** were obtained with a ~70% yield. FT-IR: 1754 (s), 1684 (m), 1336 (s), 1253 (m), 913 (s), 859 (ms), 828 (s), 645 (s), 623 (ms), 562 (s), and 497 (ms) cm^{-1}.

$[(CH_3CH_2CH_2)_4N]_2[Si(ox)_3]$ (4). Tetrapropylammonium tris(oxalato)silicate, **4**, was prepared by first combining 9.7 g of freshly prepared $Ag_2C_2O_4$ (excess) with 300 mL of dry acetone in a red glass flask. Then 1.0 mL (0.009 mol) of $SiCl_4$ and 4.65 g (0.018 mol) of $(CH_3CH_2CH_2)_4NBr$ were added. The mixture was stirred for 1 h at room temperature as the silver halides precipitated. The slurry was suction filtered, and ~400 mL of anhydrous ether was added, which resulted in precipitation of the crude product **4** in 70% yield. The crude product was dissolved in a minimum amount of absolute ethanol and stored in a refrigerator. After 48 h, colorless needles of **4** were separated from solution. FT-IR: 1754 (s), 1681 (m), 1339 (s), 1247 (m), 910 (s), 853 (ms), 826 (ms), 644 (s), 623 (ms), 563 (s), and 495 (ms) cm^{-1}.

$[(CH_3(CH_2)_3)_4N]_2[Si(ox)_3]$ (5). The synthesis of tetrabutylammonium tris(oxalato)silicate, **5**, was conducted in a similar manner to the published procedure.[5] A 4.75 g sample of freshly prepared $Ag_2C_2O_4$ (excess) were mixed with 300 mL of dry acetone in a red glass flask. Then 0.578 mL (0.005 mol) of $SiCl_4$ and 3.254 g (0.01 mol) of $(CH_3(CH_2)_3)_4NBr$ were added and stirred for 1 h at room temperature. After the precipitated silver halides were separated by suction filtration, the solution was allowed to evaporate to dryness. The solid residue was dissolved in ~200 mL absolute ethanol, gravity filtered, and evaporated with cooling to yield (55%) colorless crystals of **5**. The resulting $[(CH_3(CH_2)_3)_4N]_2[Si(ox)_3]$ crystals were hygroscopic and therefore stored in a desiccator. FT-IR: 1753 (s), 1679 (ms), 1337 (s), 1245 (ms), 909 (ms), 852 (m), 828 (ms), 644 (s), 621 (ms), 566 (s), and 496 (ms) cm^{-1}.

$[(CH_3(CH_2)_5)_4N]_2[Si(ox)_3]$ (6). Tetrahexylammonium tris(oxalato)silicate, **6**, was prepared by first mixing 5.58 g of freshly prepared $Ag_2C_2O_4$ (excess) with 300 mL of dry acetone in a red glass flask. Then 0.68 mL (0.006 mol) of $SiCl_4$ and 5.15 g (0.012 mol) of $(CH_3(CH_2)_5)_4NBr$ were added. The mixture was stirred at room temperature for 1 h. The precipitated silver halides were separated by suction filtration and the filtrate was evaporated to dryness. The crude product **6** was redissolved in absolute ethanol, filtered, and allowed to evaporate to dryness. $[(CH_3(CH_2)_5)_4N]_2[Si(ox)_3]$ can be isolated in ~50% yield as colorless triangle-shaped crystals, however, the solid is quite hygroscopic and is generally recovered as a sticky paste. FT-IR: 1764 (s), 1681 (m), 1337 (s), 1244 (ms), 911 (ms), 855 (ms), 828 (m), 645 (s), 622 (m), 565 (s), and 497 (ms) cm^{-1}.

Silicon content was determined by thermal decomposition of the samples at 500 °C. Assuming the resulting solid has the formula SiO_2 (based on spectroscopic analysis), we can compare the weight percent silicon with the expected value from the corresponding oxalate complex. In all cases the yield of silica was 100%. FT-IR spectra were obtained from KBr pellets using a Mattson 2025 FT-IR spectrophotometer. X-ray powder diffraction patterns were recorded on a Scintag XDS 2000 diffractometer using CaF_2 as an internal standard. Surface areas were measured with a Micromeritics Flowsorb II 2300 using single point procedure and a mixture of 30% by volume nitrogen in helium.

X-ray Structure Determination. Single crystals for crystallographic analysis were obtained by evaporation of an absolute ethanol solution in the vacuum oven at 60 °C and 25 Torr. The colorless, plate shaped crystals were then sealed in Lindemann capillaries. All data were collected on an Enraf-Nonius CAD-4 diffractometer $\omega-2\theta$ scan technique, Mo Kα radiation (λ = 0.710 73 Å) and a graphite monochromator. Standard procedures in our laboratory have been described previously.[6] Relevant crystallographic data and structure determination parameters for compounds **1** and **2** are listed in Table 1. Data was corrected for Lorentz and polarization effects, but not for absorption nor decay (<1% change in standard reflections measured every 3600 s of exposure time). The structures were solved by direct methods (SIR[7] (**1**) SHELX-86 (**2**))[8] and the model refined using full-matrix least-squares techniques. The treatment of thermal parameters was based on the number of observed data—anistropic parameters were incorporated for the Si and noncoordinated O atoms in **1**, but only the Si atom in **2**. Hydrogen atoms were located on difference maps, and then included in the model in idealized positions (U(H) = $1.3B_{eq}$(C)). All computations other than those specified were performed using MolEN.[9] Scattering factors were taken from the usual sources.[10]

Table 1. Crystallographic Data and Structure Determination Parameters for $[(CH_3)_4N]_2[Si(ox)_3]$ (**1**) and $[(CH_3)_3(C_6H_5)(N]_2[Si(ox)_3]$ (**2**)

$C_{14}H_{24}N_2O_{12}Si$ (**1**)	fw = 440.44
a = 17.631(2) Å	space group: $P2_1/c$
b = 10.1984(9) Å	T = ambient
c = 12.095(1) Å	λ = 0.710 73 (Å)
β = 108.810(8)°	D_{calc} = 1.421 g cm^{-3}
V = 2058.6(3) Å^3	μ = 1.69 cm^{-1}
Z = 4	R^a = 0.0631
	$R_w{}^b$ = 0.0686
$(C_{24}H_{28}N_2O_{12}Si)$ (**2**)	fw = 564.58
a = 8.855(2) Å	space group: $P2_1/n$
b = 18.050(2) Å	T = ambient
c = 17.102(2) Å	λ = 0.710 73 (Å)
β = 95.24(1)°	D_{calc} = 1.378 g cm^{-3}
V = 2722.0(6) Å^3	μ = 1.44 cm^{-1}
Z = 4	R^a = 0.0736
	$R_w{}^b$ = 0.0748

$^a R = (\sum||F_o| - |F_c||)/(\sum|F_o|)$. $^b R_w = [(w\sum||F_o| - |F_c||)^2/(w\sum|F_o|^2)]^{1/2}$.

Thermal Decomposition. Thermal decomposition of the compounds **1**−**6** was conducted under a variety of conditions which include a flow reactor, an autoclave, and a pressure reactor. Silicon oxalate samples (30−80 mg) were placed in a flow reactor and heated in a tube furnace under a stream of oxygen. Samples were heated from room temperature to 400 °C at a rate of ~1 deg min^{-1} with an extra 2 h at each 50 deg interval. The progress of decomposition was monitored by FT-IR spectroscopy. Samples thermally decomposed in a 23 mL Parr autoclave were dissolved in a mixture (~1/1, v/v) of ethylene glycol and water. The autoclave was heated under static conditions between 175 and 200 °C for 48 h. Samples were also thermally decomposed in a glass pressure reactor under variable oxygen pressures between 28 and 50 psig with reaction times of 24−100 h and a temperature range of 210−290 °C. In all cases the resulting silica was amorphous. (Note: if silver impurities are present, the crystalline Ag_2O can be detected by XRD and the silica will be discolored.)

Results and Discussion

The synthesis of a tris(oxalato)silicon complex was first reported[4] in 1969 with the preparation of $[(CH_3CH_2)_4N]_2[Si(C_2O_4)_3]$ (**3**). Subsequently, tetramethylammonium (**1**) and

(6) Mason, M. R.; Smith, J. M.; Bott, S. G.; Barron, A. R. *J. Am. Chem. Soc.* **1993**, *115*, 4971.
(7) Burla, M. C.; Camalli, M.; Cascarano, G.; Giacovazzo, C.; Polidori, G.; Spagna, R.; Viterbo, D. *J. Appl. Crystallogr.* **1989**, *22*, 389.
(8) Sheldrick, G. M. in *Crystallographic Computing*; Sheldrick, G. M., Krüger, C., Goddard, R., Eds.; OUP: Oxford, England, 1985; pp 184−189.
(9) *MolEN, An Interactive Structure Solution Program*; Enraf-Nonius: Delft, The Netherlands; 1990.
(10) Cromer, D. T.; Waber, J. T. *International Tables for X-Ray Crystallography*; Kynoch Press: Birmingham, England, 1974; Vol. IV, Table 2.

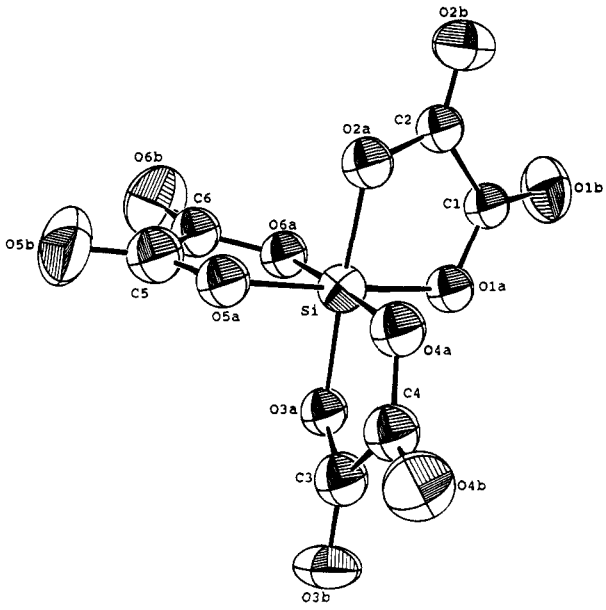

Figure 1. Molecular structure of the $Si(ox)_3^{2-}$ ion in compound **1** with atoms shown as 50% probability ellipsoids.

tetrabutylammonium (**5**) tris(oxalato) salts were synthesized using the same methodology.[5] This involves the reaction of silicon tetrachloride and an alkylammonium bromide with silver oxalate as shown in eq 1. The silver serves to remove the

$$SiCl_4 + 3Ag_2(C_2O_4) + 2R_4NBr \rightarrow 2R_4N^+Si(C_2O_4)_3^{2-} + 4AgCl\downarrow + 2AgBr\downarrow \quad (1)$$

halogens from solution as insoluble salts. In all reactions excess silver was used and recovered in subsequent purification steps. Then the silicon oxalate can be isolated by evaporating the solvent or precipitated from mixed solvents. Our efforts to control the stoichiometry of this reaction, i.e. the number of oxalate ligands coordinated to silicon, resulted only in the formation of the tris(oxalato) adducts. Similarly, replacing the ammonium salts with trialkylamines resulted in no identifiable products. The addition of amines with the ammonium ions also reduced the yield of oxalate complexes.

Compounds **3** and **5** have previously been characterized by infrared spectroscopy[4,5] with the assignments for the $Si(ox)_3^{2-}$ ion based on the assumption of D_3 symmetry. The FT-IR spectra for samples **1**−**6** in the present study are consistent with the same tris(oxalato) silicate ion proposed earlier. There are no significant shifts in the CO or SiO stretching frequencies when the charge balancing alkylammonium ion is changed. This suggests coordination of the oxalate to the silicon is unperturbed by the cation. However, the XRD patterns for samples **1**−**6** differ significantly, which indicates that the crystallographic arrangement of the $Si(ox)_3^{2-}$ anions depends on the nature of the cations. Therefore, we embarked on an effort to verify the structure of the $Si(ox)_3^{2-}$ ion and determine the effect of the cation size and shape on crystal packing. Although, samples **1**−**6** are all crystalline only the tetramethylammonium (**1**) and phenyltrimethylammonium (**2**) derivatives yielded large single crystals suitable for X-ray analysis. It would appear that as the size of the alkylammonium ion increases, the crystals become smaller and more hygroscopic, which has hampered structural characterization of compounds **3**−**6**. Nevertheless, the structures of compounds **1** and **2** are representative of the

(11) Merrachi, E. H.; Mentzen, B. F.; Chassagneux, F.; Bouix, J. *Rev. Chim. Miner.* **1987**, *24*, 56.

Table 2. Selected Bond Lengths and Angles for $[(CH_3)_4N]_2[Si(ox)_3]$ (**1**) and $[(CH_3)_3(C_6H_5)(N]_2[Si(ox)_3]$ (**2**)

bond distances (Å) for **1**		bond distances (Å) for **2**	
Si−O(1a)	1.768(9)	Si−O(1a)	1.762(9)
Si−O(2a)	1.780(9)	Si−O(2a)	1.757(9)
Si−O(3a)	1.764(8)	Si−O(3a)	1.774(9)
Si−O(4a)	1.774(7)	Si−O(4a)	1.782(9)
Si−O(5a)	1.778(9)	Si−O(5a)	1.746(9)
Si−O(6a)	1.779(7)	Si−O(6a)	1.774(9)
C(1)−O(1a)	1.31(1)	C(1)−O(1a)	1.32(2)
C(1)−O(1b)	1.20(2)	C(1)−O(1b)	1.20(2)
C(2)−O(2a)	1.30(2)	C(2)−O(2a)	1.30(2)
C(2)−O(2b)	1.19(2)	C(2)−O(2b)	1.23(2)
bond angles (deg) for 1		**bond angles (deg) for 2**	
O(1a)−Si−O(2a)	88.0(4)	O(1a)−Si−O(2a)	88.8(4)
O(1a)−Si−O(3a)	90.8(4)	O(1a)−Si−O(3a)	90.7(4)
O(1a)−Si−O(4a)	94.9(4)	O(1a)−Si−O(4a)	92.3(4)
O(1a)−Si−O(5a)	176.1(4)	O(1a)−Si−O(6a)	176.3(4)
O(1a)−Si−O(6a)	89.8(4)	O(1a)−Si−O(5a)	88.7(4)
O(2a)−Si−O(3a)	176.5(4)	O(2a)−Si−O(3a)	178.0(4)
O(2a)−Si−O(4a)	88.9(4)	O(2a)−Si−O(4a)	90.0(4)
O(2a)−Si−O(5a)	89.4(4)	O(2a)−Si−O(5a)	93.6(4)
O(2a)-Si−O(6a)	92.0(4)	O(2a)-Si−O(6a)	89.0(4)
O(3a)-Si−O(4a)	87.9(4)	O(3a)-Si−O(4a)	88.1(4)
O(3a)-Si−O(5a)	92.0(4)	O(3a)-Si−O(5a)	88.4(4)
O(3a)-Si−O(6a)	91.3(4)	O(3a)-Si−O(6a)	91.7(4)
O(4a)-Si−O(5a)	88.0(4)	O(4a)-Si−O(5a)	176.3(4)
O(4a)-Si−O(6a)	175.2(4)	O(4a)-Si−O(6a)	90.6(4)
O(5a)-Si−O(6a)	87.4(4)	O(5a)-Si−O(6a)	88.4(4)

$Si(ox)_3^{2-}$ ion and the effects of the alkylammonium ions on crystal packing can be inferred from other observations (vide infra).

Figure 1 shows the molecular structure of $Si(ox)_3^{2-}$ in compound **1** with selected bond distances and bond angles for both **1** and **2** listed in Table 2. The atom positions for compounds **1** and **2** are given in Tables 3 and 4. As anticipated three oxalate ligands coordinate to the silicon in an octahedral arrangement with near D_3 symmetry. As can be seen from Table 2 the structure of the $Si(ox)_3^{2-}$ ion in compounds **1** and **2** are nearly identical, which suggests the nature of the alkylammonium ions does not affect the silicon oxalate structure. This is further supported by the FT-IR data for compounds **1**−**6** that indicate the oxalate complexes are approximately the same. The average Si−O bond distance of 1.77(1) Å is longer than the typical range of Si−O bond distances in silicate materials (1.60−1.67 Å).[2] The C−O(a) and C−O(b) distances are consistent with the bound oxygens (a) (1.31 Å) and unbound oxygens (b) (1.20 Å) having single bond and double bond character respectively. These can be compared to the C−O distances in the related compound[11] $[NH_4]_3[Fe(C_2O_4)_3]\cdot 3H_2O$, where the average C−O distance for bound oxygens was 1.276 Å and for terminal oxygens 1.223 Å. The apparent greater polarization of the oxalate ligand in $Si(ox)_3^{2-}$ probably arises from the higher electrostatic potential associated with Si^{4+}. The O−Si−O bond angles are slightly smaller than 90° for the 5 membered ring formed by the chelate with an average 87.8° and 88.4° for compounds **1** and **2**, respectively. Between oxalate ligands the O−Si−O angles are on average slightly larger with 90.9° for complex **1** and 90.5° for complex **2**. These results can be compared with $Fe(ox)_3^{3-}$ where the average O−Fe−O angle for the chelate was 80.4° and as high as 105.9° between two of the ligands.[11]

Although the difference between tetramethylammonium and phenyltrimethylammonium ions apparently does not affect the structure of the $Si(ox)_3^{2-}$ ion, the size of the cation alters the arrangement of the oxalate complexes. Figures 2 and 3 show the unit cells for $[(CH_3)_4N]_2[Si(ox)_3]$ (**1**) and $[(CH_3)_3(C_6H_5)N]_2$-

Table 3. Positional Parameters and Their Estimated Standard Deviations for Phenyltrimethylammonium Tris(oxalato)silicate

atom	*x*	*y*	*z*	*B*, Å^2
Si	1.0006(4)	0.3853(2)	0.2245(2)	3.46(8)
O1a	1.1362(9)	0.3550(5)	0.1623(5)	4.3(2)*
O1b	1.330(1)	0.3966(6)	0.1015(6)	7.3(3)
O2b	1.271(1)	0.5349(6)	0.1766(6)	6.0(2)
O2a	1.0814(9)	0.4742(4)	0.2236(5)	3.9(2)*
O3b	0.716(1)	0.2371(6)	0.1639(6)	6.8(3)
O3a	0.9163(9)	0.2961(5)	0.2219(5)	4.3(2)*
O4b	0.684(1)	0.3617(5)	0.0610(6)	6.5(3)
O4a	0.8696(9)	0.4102(5)	0.1435(5)	4.2(2)*
O5b	1.129(1)	0.3450(60	0.4360(6)	6.4(3)
O5a	1.1217(9)	0.3561(5)	0.3049(5)	4.1(2)*
O6a	0.8740(9)	0.4182(4)	0.2913(5)	3.6(2)*
O6b	0.845(1)	0.4186(6)	0.4181(6)	6.7(3)
N11	0.865(1)	0.1125(6)	0.3705(6)	3.7(2)*
N21	0.844(1)	0.3460(6)	0.6248(6)	3.7(2)*
C1	1.230(1)	0.4073(8)	0.1436(8)	4.6(3)*
C2	1.195(1)	0.4781(8)	0.1801(8)	4.3(3)*
C3	0.798(1)	0.2918(7)	0.1700(8)	4.4(3)*
C4	0.777(1)	0.3585(7)	0.1188(7)	3.8(3)*
C12	0.695(2)	0.2207(8)	0.3672(8)	5.2(3)*
C13	0.556(2)	0.254(1)	0.384(1)	7.4(5)*
C14	0.456(2)	0.215(1)	0.418(1)	7.2(4)*
C15	0.471(2)	0.144(1)	0.435(1)	7.7(5)*
C16	0.612(2)	0.1066(9)	0.4193(9)	5.8(4)*
C17	0.847(2)	0.0835(9)	0.288(1)	6.8(4)*
C18	0.992(2)	0.165(1)	0.378(1)	7.1(4)*
C19	0.904(2)	0.0500(9)	0.4243(9)	6.6(4)*
C21	0.693(1)	0.3819(7)	0.6083(7)	3.6(3)*
C22	0.675(2)	0.4565(9)	0.6216(9)	6.2(4)*
C23	0.528(2)	0.487(1)	0.607(1)	7.3(4)*
C24	0.416(2)	0.4451(9)	0.582(1)	6.7(4)*
C25	0.425(2)	0.373(1)	0.569(1)	7.9(5)*
C26	0.566(2)	0.3407(9)	0.5858(9)	6.0(4)*
C27	0.852(2)	0.3135(8)	0.7045(9)	5.5(4)*
C28	0.867(2)	0.2864(8)	0.5660(8)	4.8(3)*
C29	0.971(2)	0.3992(8)	0.6199(9)	5.7(4)*

[a] Starred values denote atoms that were refined isotopically. Values for anisotropically refined atoms are given in the form of the isotropic equivalent displacement parameter defined as: $(4/3)[a^2B(1,1) + b^2B(2,2) + c^2B(3,3) + ab(\cos\gamma)B(1,2) + ac(\cos\beta)B(1,3) + bc(\cos\alpha)B(2,3)]$.

Table 4. Positional Parameters and Their Estimated Standard Deviations for Tetramethylammonium Tris(oxalato)silicate

atom	*x*	*y*	*z*	*B*, Å^2
Si	0.2500(2)	0.1545(4)	0.0832(3)	3.26(7)
O1a	0.3136(4)	0.2165(7)	0.0086(6)	3.7(2)*
O1b	0.3943(5)	0.142(1)	−0.0861(7)	5.9(3)
O2a	0.2498(4)	0.0021(9)	0.0114(6)	3.9(2)*
O2b	0.3141(5)	−0.1019(9)	−0.0899(7)	5.5(2)
O3a	0.2466(4)	0.3095(7)	0.1460(6)	3.4(2)*
O3b	0.1667(5)	0.4795(8)	0.1348(7)	5.2(2)
O4a	0.1599(4)	0.1966(8)	−0.0282(6)	4.1(2)*
O4b	0.0632(5)	0.350(1)	−0.0692(7)	5.8(2)
O5a	0.1904(4)	0.0826(8)	0.1610(6)	4.0(2)*
O5b	0.2031(6)	−0.019(1)	0.3307(8)	8.1(3)
O6a	0.3355(4)	0.1088(8)	0.2024(6)	3.8(2)*
O6b	0.3709(6)	−0.013(1)	0.3643(8)	7.5(3)
N11	0.0660(5)	0.7795(9)	−0.1231(8)	3.4(2)*
N21	0.4199(5)	0.6218(9)	0.1748(7)	3.6(2)*
C1	0.3420(6)	0.126(1)	−0.0436(9)	3.4(3)*
C2	0.3018(6)	−0.005(1)	−0.0440(9)	3.5(3)*
C3	0.1814(7)	0.376(1)	0.099(1)	4.2(3)*
C4	0.1272(7)	0.307(1)	−0.012(1)	4.1(3)*
C5	0.2295(7)	0.033(1)	0.260(1)	4.9(3)*
C6	0.3215(7)	0.038(1)	0.285(1)	4.2(3)*
C11	0.1075(8)	0.830(1)	−0.201(1)	5.7(3)*
C12	0.0178(8)	0.663(2)	−0.175(1)	6.3(4)*
C13	0.0133(9)	0.880(2)	−0.107(1)	7.8(4)*
C14	0.1262(9)	0.746(2)	−0.011(1)	7.2(4)*
C21	0.4592(8)	0.653(2)	0.299(1)	6.3(4)*
C22	0.4297(9)	0.479(2)	0.158(1)	7.9(5)*
C23	0.3327(9)	0.647(2)	0.140(1)	8.1(5)*
C24	0.4559(8)	0.697(1)	0.099(1)	5.5(3)*

[a] Starred values denote atoms that were refined isotropically. Values for anisotropically refined atoms are given in the form of the isotropic equivalent displacement parameter defined as: $(4/3)[a^2B(1,1) + b^2B(2,2) + c^2B(3,3) + ab(\cos\gamma)B(1,2) + ac(\cos\beta)B(1,3) + bc(\cos\alpha)B(2,3)]$.

$[Si(ox)_3]$ (**2**) respectively. The $Si(ox)_3^{2-}$ ions form layers that are linked by the alkylammonium ions. We have measured C-H···O distances as close as 2.4 Å in both structures, which indicates some degree of hydrogen bonding. It is clear from Figure 3 that the larger phenyltrimethylammonium ion forces the oxalate complexes to be spaced further apart. We expect the larger cations in compounds **3**−**6** to spread the lattice out even further. The iron oxalate anions in $[NH_4]_3[Fe(C_2O_4)_3]\cdot 3H_2O$ arrange themselves to form channels that include the ammonium ions and water.[11] Closer examination of an extended lattice of compound **2** also reveals a channel like arrangement. Figure 4 shows a view down the *a* axis of the $Si(ox)_3^{2-}$ ions only in compound **2** which illustrate the elliptical shaped voids that are defined by the anions. The cations not shown occupy this space. The packing of molecules in compound **1** was too dense to resolve any obvious pore structure.

We originally had envisioned silicon oxalates with such preorganized pore structures as potential precursors to new and interesting silicate materials. The silicon oxalates should decompose to silica at ~300 °C[3,5] while the ammonium ions are converted to amines. We reasoned that the ammonium ions or amines might function as templates under the right conditions to form a crystalline silica phase that reflects the pore structure of the oxalate precursor. Unfortunately, the thermal decomposition of **1**−**6** has only resulted in amorphous silica so far. The silicon oxalate complexes will hydrolyze in water so we first attempted the heating the samples in a mixture of ethylene glycol and water under static conditions in a Paar reactor. However, all the products were amorphous. Next we attempted to heat the silicon oxalate crystals under oxygen pressure but again the resulting materials were amorphous. Heating the samples under a flow of oxygen and/or steam also produced amorphous silica. The silicon oxalate complexes were not heated above 500 °C but we would expect as the temperature is increased the likelihood that crystalline, microporous materials would form diminishes.

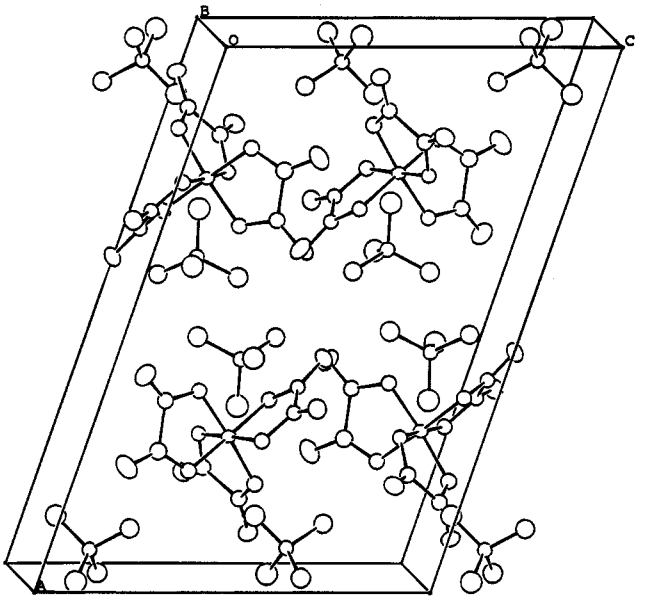

Figure 2. Unit cell for $[(CH_3)_4N]_2[Si(ox)_3]$ (**1**) with hydrogens omitted for clarity.

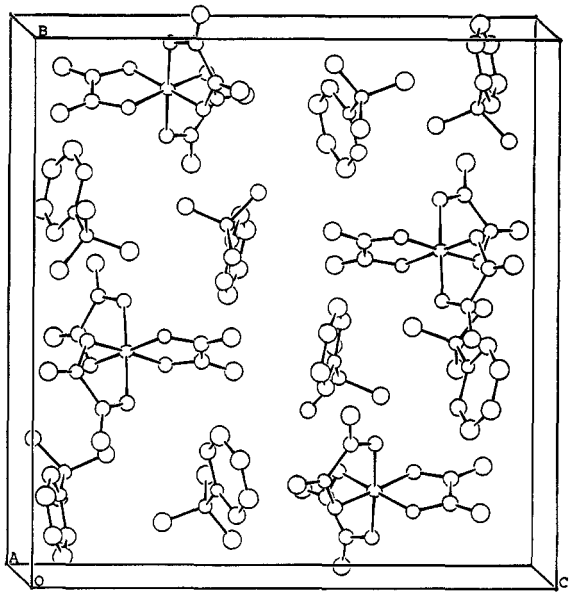

Figure 3. Unit cell for $[(CH_3)_3(C_6H_5)N]_2[Si(ox)_3]$ (**2**) with hydrogens omitted for clarity.

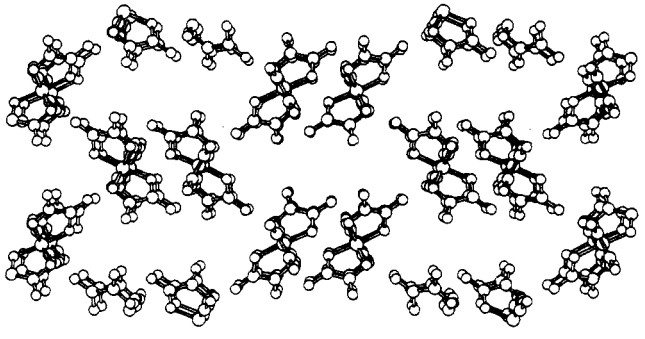

Figure 4. Packing arrangement of $Si(ox)_3^{2-}$ ions in compound 2 viewed down the *a* axis.

Although the resulting silica products were amorphous the surface area was significantly different for samples **1**−**6**. The series of silicon oxalates (**1**−**6**) were all decomposed under the same conditions under a flow of oxygen in a tube furnace at 400 °C. Then a single point surface area was determined for the silica products. Figure 5 shows a plot of surface area vs the C/N ratio in the alkylammonium ion in each compound. These values are tentative, because they represent single points on the adsorption isotherms. However, a clear trend in surface area emerges with alkylammonium ion size. As the C/N ratio increases the surface area increases, such that heating compound **5** results in silica with more than twice the surface area of compound **1**. This was anticipated because of the steric requirements of the larger alkylammonium salts. Figure 6 shows the calculated structures of the alkylammonium ions associated with compounds **1**−**6** using VDW radii. We know from the crystallographic study of compounds **1** and **2** that the steric requirements of the phenyltrimethylammonium ion result in a less dense arrangement of $Si(ox)_3^{2-}$ ions. It should be obvious from this figure that the size of the cation increases with C/N ratio which should systematically increase the porosity of the silicon oxalate sublattice. We propose this manifests itself in the surface areas of the silica prepared by thermal decomposition of the oxalates.

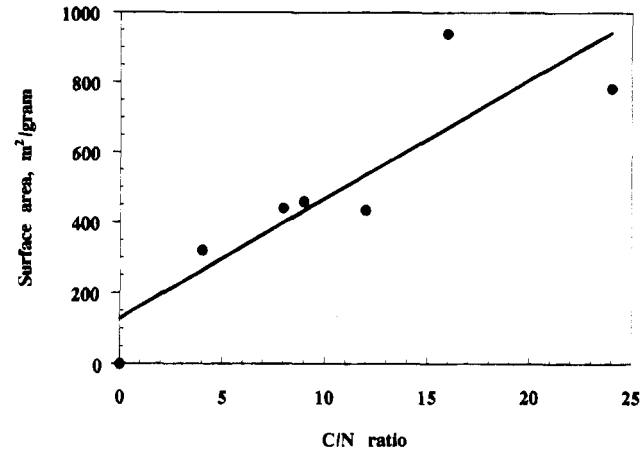

Figure 5. Plot of surface area (m^2/g) vs the C/N for the alkylammonium cations in compounds **1**−**6**.

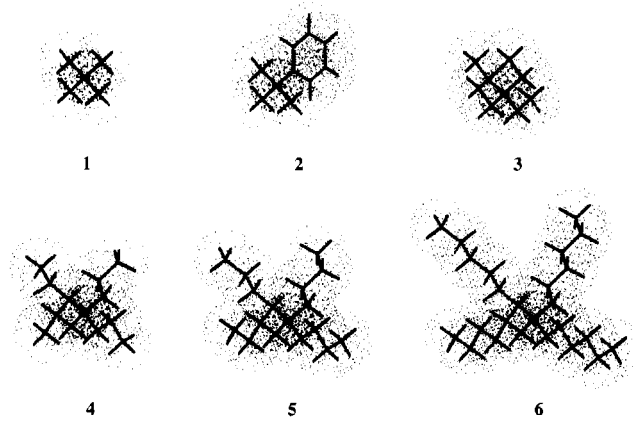

Figure 6. Calculated structures of alkylammonium cations in compounds **1**−**6** using CAChe molecular modeling and MM2 parameters. The cations are shown with VDW radii.

Conclusions

We have crystallographically verified the octahedral arrangement of oxalate ligands around silicon in $Si(ox)_3^{2-}$ for two different alkylammonium salts. These structures reveal the effect of cation size on packing arrangement of silicon oxalate anions. This can be exploited in the preparation of metal oxides with controlled porosity. The thermal decomposition of silicon oxalates would be a complex and expensive route to high surface area silica. Nevertheless, we have demonstrated that we can prepare silica with surface areas approaching 1000 $m^2\ g^{-1}$ using silicon oxalates as precursors. The issue of whether we can obtain crystalline oxide materials from silicon oxalates remains a subject of interest.

Acknowledgment. We would like to thank the National Science Foundation (Grant CHE-9157014) and the Robert A. Welch Foundation (K.J.B., S.G.B.) as well as the UNT Research Office for their financial support.

Supporting Information Available: Tables of crystal and refinement data, hydrogen atom parameters, general displacement parameter expressions—*U*'s, bond distances, bond angles, torsion angles, and least-squares planes (30 pages). Ordering information is given on any current masthead page.

IC950552W